Published in final edited form as:
Life Sci. 2012 September 4; 91(0): 199–206. doi:10.1016/j.lfs.2012.07.010.

Humanin prevents intra-renal microvascular remodeling and inflammation in hypercholesterolemic ApoE deficient mice

Xin Zhang[1], **Victor H. Urbieta-Caceres**[1], **Alfonso Eirin**[1], **Caitlin C. Bell**[1], **John A. Crane**[1], **Hui Tang**[1], **Kyra Jordan**[1], **Yun-Kyu Oh**[2], **Xiang-Yang Zhu**[1], **Michael J. Korsmo**[1], **Adi R. Bachar**[2], **Pinchas Cohen**[3], **Amir Lerman**[2], and **Lilach O. Lerman**[1,2]

[1]Division of Nephrology and Hypertension, Mayo Clinic, Rochester, MN, 55905

[2]Division of Cardiovascular Diseases, Mayo Clinic, Rochester, MN, 55905

[3]Department of Pediatrics, Division of Endocrinology, UCLA, 405 Hilgard Avenue, Los Angeles, CA, 90095

Abstract

Aims—Humanin (HN) is endogenous mitochondrial-derived cytoprotective peptide that has shown protective effects against atherosclerosis and is expressed in human vessels. However, its effects on the progression of kidney disease are unknown. We hypothesized that HN would protect the kidney in the early phase of atherogenesis.

Main methods—Forty-eight mice were studied in four groups (n=12 each). Twenty-four ApoE deficient mice were fed a 16-week high-cholesterol diet supplemented with saline or HN (4 mg/kg/day, intraperitoneal). C57BL/6 mice were fed a normal diet supplemented with saline or HN. Microvascular architecture was assessed with micro-CT and vascular wall remodeling by alpha-SMA staining. The effects of HN on angiogenesis, inflammation, apoptosis and fibrosis were evaluated in the kidney tissue by Western Blotting and histology.

Key findings—Cortical microvascular spatial density and media/lumen area ratio were significantly increased in high-cholesterol diet fed ApoE deficient mice, but restored by HN. HN up-regulated the renal expressions of anti-angiogenic proteins angiostatin and TSP-1, and inhibited angiopoietin-1. HN attenuated inflammation by down-regulating MCP-1, TNF-alpha and osteopontin. HN also tended to restore pSTAT3 and attenuated Bax expression, suggesting blunted apoptosis. Kidney collagen IV expression was alleviated by HN treatment.

Significance—HN attenuates renal microvascular remodeling, inflammation and apoptosis in the early stage of kidney disease in hypercholesterolemic ApoE$^{-/-}$ mice. HN may serve as a novel therapeutic target to mitigate kidney damage in early atherosclerosis.

Keywords

humanin; hypercholesterolemia; angiogenesis; inflammation; kidney disease

Correspondence: Lilach O. Lerman, MD, PhD, Division of Nephrology and Hypertension, Mayo Clinic, 200 First Street SW, Rochester, MN 55905. Fax: (507)-266-9316, Phone: (507)-266-9376, lerman.lilach@mayo.edu.

Disclosures
No conflicts of interest, financial or otherwise, are declared by the author(s).

1. Introduction

Chronic kidney disease (CKD) is associated with a high incidence of cardiovascular morbidity and mortality, and renal dysfunction due to CKD correlates with a striking increase in cardiovascular events. Atherosclerosis, a generalized inflammatory vascular disease, is an important contributor to the development and progression of CKD and constitutes one of the major causes of morbidity and mortality in CKD. (Collins et al. 2003)

Atherosclerosis is associated with a series of cellular and molecular responses to endogenous and exogenous insults, resembling those triggered in other forms of CKD, including oxidative stress, inflammation, and vascular remodeling.(Oberg et al. 2004) We have previously shown that hypercholesterolemia, considered a surrogate for early atherosclerosis, (Chade et al. 2005a) developed kidney microvascular proliferation in pigs, probably secondary to renal inflammation.(Chade et al. 2007) Furthermore, in atherosclerosis oxidized low-density lipoprotein (Ox-LDL) induces endothelial cell dysfunction and injury, infiltrates the mesangium and blood vessels, and subsequently promotes secretion of growth factors that lead to glomerular and vascular hypercellularity and proliferation of extracellular matrix. (Chade et al. 2005b)

Humanin (HN) is an endogenous mitochondrial-derived metabolo-protective/cytoprotective peptide consisting of 24 amino acid residues. Its ability to blunt apoptosis has been established in Alzheimer's disease, (Hashimoto et al. 2001) and in other organs such as pancreatic endocrine beta-cells.(Hoang et al. 2010) HN exerts its action by interfering with the pro-apoptotic factor Bax,(Guo et al. 2003) interacting with IGF binding protein 3 (IGFBP3),(Ikonen et al. 2003) and inhibiting signal transducer and activator of transcription 3 (STAT3).(Hoang et al. 2010) In addition to anti-apoptotic properties, we have previously shown that HN also reduced both Ox-LDL-induced reactive oxygen species formation and apoptosis in endothelial cells, and is expressed in the human aorta as well as in carotid atherosclerotic plaques.(Bachar et al. 2010); (Zacharias et al. 2012) These findings highlight the ability of HN to exert cytoprotective effects through diverse mechanisms and mitigate vascular damage during the development of atherosclerosis. We recently found that a 16-week treatment with a humanin analogue prevents the development of atherosclerotic plaques in the aorta of ApoE deficient ($ApoE^{-/-}$) mice.(Oh et al. 2011) However, the potential effects of HN on kidney injury in early atherosclerosis have not been elucidated. We hypothesized that HN would protect kidney vessels from atherosclerotic insults, and explored the effects of HN supplementation on intra-renal microvascular architecture, inflammation, and apoptosis in hypercholesterolemic $ApoE^{-/-}$ mice.

2. Materials and methods

2.1 Experimental protocol

The study was approved by the Mayo Clinic Institutional Animal Care and Use Committee. Twenty-four female C57BL/6 and 24 $ApoE^{-/-}$ mice (4 weeks old) were obtained from Jackson Laboratory. All the animals had free access to water, were maintained at 24°C, and kept at a 12hr light/dark cycle. C57BL/6 mice were then fed with a normal diet (standard chow), while $ApoE^{-/-}$ mice were fed with high-cholesterol diet (0.15% cholesterol and 42% milk fat by weight, TD88137; Harlan Teklad) to precipitate development of atherosclerosis. (Plump et al. 1992) In addition, the C57BL/6 and $ApoE^{-/-}$ mice were randomized to 16 weeks of intraperitoneal (IP) injections of either saline vehicle (Control, n=12, and $ApoE^{-/-}$, n=12) or the HN-analogue HN-glycine (0.4 mg/kg/day,10 Peptide International, Louisville, KY, Control+HN, n=12, and $ApoE^{-/-}$+HN, n=12), a ×1,000 more potent variant of HN. (Hashimoto et al. 2001)

At the end of 16 weeks, animals were anaesthetized and euthanized with 100 mg/kg of ketamine and 10 mg/kg of xylazine IP in a prone position on an animal tray. Blood samples were collected by cardiac puncture. Laparotomy was performed, and kidneys randomly either perfused with a contrast agent through the aorta for micro-CT (n=6) or isolated and prepared for renal tissue studies (n=6). One kidney was studied per mouse.

2.2 Plasma lipid and renal function measurements

Blood samples were immediately transferred to EDTA tubes, centrifuged at 5,000 rpm for 10 min, and kept at −80°C until determination of lipid profiles (Roche), serum creatinine (spectrophotometry), blood urea nitrogen (BUN, ELISA), and plasma renin concentration (PRC, RIA).

2.3 Micro-CT

A ligature was placed and a cannula inserted in the aorta proximal to the renal arteries, and the aorta distal to the renal artery as well as arterial branches to the liver and bowels were ligated. Because of the small size of the renal artery that precludes catheterization, the aorta and both kidneys then perfused with heparinized saline, and the renal veins cut to allow venous drainage. This kidneys were then infused with an intravascular contrast agent (0.8 ml/min), a radio-opaque silicone polymer (Microfil MV122, Flow Tech, Carver, MA), until the kidneys had a uniform yellow coloration and the polymer drained freely from the renal veins. At the end of infusion the renal arteries and veins were ligated, the kidneys removed, immersed in 10% formalin, and embedded in a synthetic resin for Micro-CT scanning. One kidney per animal was scanned with micro-CT.

The kidneys were scanned at 0.5° increments using a micro-CT scanner, as described previously.(Zhu et al. 2004) Three-dimensional 20μm on-a-side images were then reconstructed and analyzed with the Analyze™ software package (Analyzer 10.0, Biomedical Imaging Resource, Mayo Clinic, Rochester, MN).(Chade et al. 2006) The cortex was tomographically divided into 10 levels at equal intervals, and the spatial density of cortical microvessels calculated in each level and averaged. The 300 micro-meters (μm) represented the largest microvessels observed within the mouse cortex, and were further categorized as small (<150 μm) or large (150~300 μm) microvessels. To correct for elliptical vessels showing lengthwise in the plane of the image, circularity and rectangularity limits built within Analyze™ were applied to exclude objects that were not truly cross-sectional.

2.4 Western blotting for kidney tissue

Standard blotting protocols were followed, as described (Chade et al. 2003), to examine protein expression of angiogenesis, apoptosis, and inflammation mediators in renal tissue. Specific antibodies against vascular endothelial growth factor (VEGF, 1:200 Santa Cruz), VEGF receptor-2 (FLK-1, 1:200, Santa Cruz), angiopoietin-1 (1:200, Santa Cruz), angiostatin (1:500, abcam) and thrombospondin 1 (TSP-1, 1:500, abcam) were used to evaluate the angiogenesis pathway; total and phosphorylated signal transducer and activator of transcription-3 (pSTAT3, both 1:1000, Cell Signaling Technology, Beverly, MA), Bax and Bcl-xL (both 1:200, Santa Cruz) to examine apoptosis activity; monocyte chemotactic protein-1 (MCP-1, 1:500, BioVision, CA), tumor necrosis factor-alpha (TNF-alpha, 1:200 abcam) to examine inflammation, and osteopontin (1:1000, abcam) for both inflammation and angiogenesis. (Asou et al. 2001); (Scatena et al. 2007) Horseradish peroxidase secondary antibodies (GE Healthcare UK Limited) were used and chemiluminescence determined using the SuperSignal West Pico Chemiluminescent Substrate or SuperSignal West Femto Maximum Sensitivity Substrate (Thermo Scientific, IL) according to vendor's instructions. Glyceraldehyde 3-phosphate dehydrogenase (GAPDH, 1:5,000 Covance, Emeryville, CA) served as loading control.

The intensity of the protein bands (one per animal) was quantified using the Alpha-Imager 3400 software (Alpha Innotech Corp., San Leandro, CA), and expressed as relative intensity units normalized to GAPDH (except for pSTAT3/total STAT3), and averaged in each group.

2.5 Histology

Midhilar 5μm cross-sections of each kidney (1 per animal) were used for histology, as described.(Zhu et al. 2009) Collagen-IV (1:50 abcam) for renal fibrosis was semi-automatically quantified in 10 randomly-selected fields from both cortex and medulla in each representative slide using a computer-aided image-analysis program (AxioCam® digital camera, AxioObserver.Z1 and AxioVision® software v4.7.2.0, Carl Zeiss MicroImaging, Inc., Thornwood, NY). The quantification of each field was expressed as percentage positive staining of total surface area, and the results from all fields in each slide averaged. Immunoreactivity of MCP-1 (1:10, MYBioSource), TNF-alpha (1:200, NOVUS, CO) and the macrophage marker F4/80 (1:50, abcam) for intra-renal inflammation was also evaluated. Apoptotic cells were detected by the Terminal dUTP nick end-labeling (TUNEL) test (ApopTag peroxidase in-situ apoptosis detection kit, Serologicals Corp), and similarly quantified in 15 fields per slide. To evaluate microvascular wall remodeling, alpha-smooth muscle actin (alpha-SMA, 1:50 abcam) staining was performed, with the secondary antibody, IgG Envision Plus (Dako, Carpenteria, CA, USA) followed by staining with the Vector NovaRED substrate kit (Vector Laboratories, Burlingame, CA). Cortical vessels (5–10) from each slide were randomly selected, and Analyze™ used to trace the inner and outer perimeters of the media layer to calculate the media and lumen areas. The extent of vascular remodeling of each vessel was represented as the media to lumen areas ratio, (Sparks et al. 2011) and was then averaged.

2.7 Statistical analysis

Statistical analysis was performed using JMP software package version 8.0 (SAS Institute Inc. Cary, NC). Shapiro-Wilk test was used to examine the deviation from normality. Normally distributed variables were expressed as mean ± SEM. Comparisons among groups were performed using ANOVA, followed by unpaired Student's t-test with the Bonferroni correction. Comparisons within and among the groups were performed using non-parametric tests (Wilcoxon and Kruskal Wallis, respectively). Statistical significance was accepted at $P < 0.05$.

3. Results

3.1 Mice characteristics

After 16 weeks, ApoE$^{-/-}$ mice had higher body weight and plasma cholesterol levels than controls (both $P<0.01$). BUN was slightly elevated in ApoE−/− mice (normal values in mice are ≤42mg/dl according to vendor protocol) compared to C57BL/6 and unaffected by HN, while serum creatinine was comparable among the groups. Incidentally, PRC in ApoE$^{-/-}$ was lower than Control (Table 1).

3.2 Microvascular 3D architecture and vascular wall remodeling

The average spatial density of cortical microvessels was significantly increased in the ApoE$^{-/-}$ group ($P<0.05$ vs. Control) in small microvessels (diameters<150 μm), but restored by HN ($P<0.05$ vs. ApoE$^{-/-}$, Figure 1, A–D, E1–2). Alpha-SMA staining showed that the media/lumen area ratio in cortical microvessels was significantly elevated in ApoE$^{-/-}$ ($P=0.04$ vs. Control), suggesting vascular wall remodeling, which was also preserved by HN ($P<0.05$ vs. ApoE$^{-/-}$) (Figure 1, F–J).

To explore the mechanism through which HN improved microvascular architecture, the activity of angiogenic and anti-angiogenic proteins was examined. VEGF expression was attenuated in ApoE$^{-/-}$ kidneys (P<0.01 vs. Control) and restored in ApoE$^{-/-}$+HN (P<0.01 vs. ApoE$^{-/-}$), as was FLK-1 (P<0.05 vs. ApoE$^{-/-}$, Figure 2). HN inhibited Angiopoietin-1 in ApoE$^{-/-}$ (Figure 2). However, the expression of the anti-angiogenic proteins angiostatin and TSP-1 was notably upregulated in both HN-treated groups (Figure 3A). Angiostatin was also elevated in untreated ApoE$^{-/-}$ mice, possibly in compensation for the increased microvascular density.

3.3 Intra-renal inflammation

MCP-1 protein expression was significantly augmented in ApoE$^{-/-}$ (P<0.05) but not in ApoE$^{-/-}$+HN, and HN downregulated TNF-alpha in ApoE$^{-/-}$ +HN compared to both Control and ApoE$^{-/-}$, although it was not elevated in ApoE$^{-/-}$ (Figure 3A). HN also inhibited osteopontin in ApoE$^{-/-}$ (Figure 3A). This was further confirmed by MCP-1 and TNF-alpha stainings, which demonstrated increased expression in ApoE$^{-/-}$ that was normalized by HN (P<0.05 vs. ApoE$^{-/-}$, Figure 3B). An increase in ApoE$^{-/-}$ mice in F4/80+ macrophages, which are often recruited in response to pro-inflammatory chemokines, was also normalized by HN (Figure 3B).

3.4 Intra-renal apoptosis

TUNEL staining revealed a significant increase in the number of apoptotic cells in ApoE$^{-/-}$ compared to Control (P<0.05), but not in ApoE$^{-/-}$+HN (Figure 4, A–D and E). In immunofluorescent images, apoptotic cells appeared to be mainly localized in tubulo-interstitial areas. pSTAT3 declined in ApoE$^{-/-}$ but not in HN, and Bax was markedly reduced in ApoE$^{-/-}$ +HN compared to both Controls and ApoE$^{-/-}$ (both P<0.01), suggesting blunted apoptotic activity of HN. Bcl-xL expression was similar among the groups (Figure 4).

3.5 Renal fibrosis

Collagen IV staining in both the cortex and medulla was increased in ApoE$^{-/-}$ mice compared to Control and blunted in ApoE$^{-/-}$+HN (Figure 5).

4. Discussion

This study shows that HN prevented pathological renal microvascular remodeling, attenuated inflammation, and reduced apoptosis in early atherosclerosis represented by the combination of ApoE deficiency and hypercholesterolemia. To our knowledge, this is the first report demonstrating a beneficial effect of HN in high cholesterolemia-induced chronic kidney disease.

Abundant evidence from our previous work and others has implicated neovascularization and microvascular wall remodeling as key processes in the early stage of atherosclerosis in the kidney(Chade et al. 2007);(Bentley et al. 2002) and heart,(Zhu et al. 2004) possibly as a compensatory mechanism to maintain basal renal hemodynamics and vascular function. (Chade et al. 2007) Inflammatory factors triggered in atherosclerosis play an important role in angiogenesis. By releasing cytokines and growth factors, inflammatory cells induce new vessel growth via stimulating the expression of pro-angiogenic factors such as VEGF. (Salomonsson et al. 2002) Furthermore, low amounts of reactive oxygen species and Ox-LDL also trigger neovascularization.(Dandapat et al. 2007)

Interestingly, despite evident microvascular proliferation, expression of VEGF and its receptor FLK-1 was downregulated in the ApoE$^{-/-}$ kidneys. VEGF is a key component

responsible for angiogenesis, which is often expressed during renal neovascularization in early atherosclerosis. (Bentley et al. 2002); (Chade et al. 2007) However, we have observed that its upregulation is transient, and VEGF expression subsequently declines under chronic conditions.(Chade et al. 2006) These data can be interpreted to indicate that at an earlier stage of hypercholesterolemia, angiogenesis was triggered due to inflammation or hypoxia through upregulation of VEGF expression, which might have been subsequently suppressed as a negative feedback once neovascularization was fully developed. This contention is supported by the parallel downregulation of FLK-1. Furthermore, this negative feedback mechanism was accompanied by stimulation of anti-angiogenic factors (angiostatin) in order to contain angiogenesis. HN, in turn, inhibited neovascularization by upregulating both angiostatin and TSP-1 and inhibiting angiopoietin-1 and osteopontin that facilitate angiogenesis, (Asou et al. 2001) followed by restoration of VEGF, possibly to sustain vascular density at an optimal functional level. The present study therefore underscores the delicate balance between pro- and anti-angiogenic factors responsible for regulating angiogenesis.(Moreno et al. 2006)

In the current study, we also observed increased expression of MCP-1 and TNF-alpha in ApoE$^{-/-}$ mice kidneys, suggesting inflammation in early atherosclerosis. MCP-1 can induce an influx of inflammatory cells like macrophages (represented by F4/80 in our study) and angiogenesis by activating its receptors CCR-2 on endothelial cells.(Salcedo et al. 2000) TNF-alpha is a well-known inflammatory and pro-angiogenic factor,(Ligresti et al. 2011) and osteopontin aids in recruitment of monocytes-macrophages and to regulate their cytokine production, (Scatena et al. 2007) which was consistent with influx of F4/80 positive cells. The significant downregulation of MCP-1, TNF-alpha and osteopontin in ApoE$^{-/-}$ +HN kidneys, along with the fewer F4/80+ cells, underscores the anti-inflammatory properties of HN. Similarly, in cognitive-deficient mice HN inhibited TNF-alpha and other inflammatory factors.(Miao et al. 2008) The association of intra-renal microvascular density and expression of pro-angiogenic inflammatory factors in this study extends our previous observations linking inflammation to intra-renal angiogenesis associated with early atherosclerosis. It is thus likely that HN attenuated angiogenesis at least partly by blunting inflammation.

The present study introduces a potential novel mechanism for HN in blunting neovascularization through activation of anti-angiogenic factors. As neo-vessels may act as conduits for leukocyte exchange, (Moulton et al. 2003) inhibition of angiogenesis by HN may further decrease local accumulation of inflammatory cells, and thereby ameliorate the progression of both atherosclerosis and nephropathy.

In addition to the increase in the number of apoptotic cells, enhanced renal apoptotic activity was disclosed by reduced expression of pSTAT3 in ApoE$^{-/-}$. The mechanism by which renal apoptosis is activated in early atherosclerosis has not been fully clarified, but downregulation of STAT3, as we observed in ApoE$^{-/-}$ kidneys, and upregulation of Bax, may play important roles. (Wang et al. 2008);(Yeh et al. 2011) Although STAT3 activation was not significantly higher in ApoE$^{-/-}$+HN than in untreated ApoE$^{-/-}$, unlike the latter STAT3 in ApoE$^{-/-}$+HN was also not significantly lower than in Controls, suggesting that HN partly blunted downregulation of STAT3 activity this group. This may in turn translate into increased availability of several anti-apoptotic molecules, including survivin, Bcl-xL, Bcl-2, and Mcl-1, downstream targets of STAT3.(Amin et al. 2004) Furthermore, HN also directly binds to Bax, a key apoptosis-inducing protein, stabilizes its conformation, and suppresses its translocation from the cytosol to mitochondria, thereby preventing cytochrome-c release, (Guo et al. 2003) and in turn inhibiting caspase-3 activation and consequent cell death. Indeed, the observed downregulation of Bax in HN-treated ApoE$^{-/-}$ mice is in agreement with this mechanism of action attributed to HN.

Collagen IV was markedly increased in the renal cortex and medulla of ApoE$^{-/-}$ mice, suggesting a tendency to develop fibrosis. However, serum creatinine was unchanged in ApoE$^{-/-}$ mice, suggesting preserved renal function, as commonly observed in animal models and humans with early atherosclerosis.(Chade et al. 2002); (Wuerzner et al. 2010) Nevertheless, we cannot rule out some impairment of renal function that HN did not correct, including slightly elevated BUN in ApoE$^{-/-}$ mice, although it might potentially be related to their diet.

In this study, we used a previously established dose of HN, which was effective in preventing development of atherosclerotic plaques in the ApoE$^{-/-}$ mice aorta. (Oh et al. 2011) However, the physiological level of HN, the effective dosage and duration of HN treatment in human with hypercholesterolemia and atherosclerosis is yet unclear. Evaluation of renal function was limited to serum creatinine and BUN, while early chronic kidney disease indices like creatinine clearance, proteinuria, or urine albumin/creatinine ratio were not available. Our study is also limited by the lack of blood pressure data, which could affect renal injury, yet no studies have attributed to HN direct vasoactive properties. The mechanism of the decrease PRC observed in Apo E$^{-/-}$ mice is unclear and warrants further studies. Future studies will also need to delineate potential receptors and pathways involved in HN's action in kidneys.

4. Conclusion

In summary, we demonstrated for the first time that exogenous supplementation of HN confers a benefit against murine kidney injury associated with high cholesterolemia, a surrogate for early atherosclerosis. The mechanisms involved likely include attenuation of pathological angiogenesis, inflammation, and apoptosis. This study therefore suggests HN as a protective strategy to blunt atherogenic kidney disease. Further studies are needed to elucidate the potentially protective role of HN in other forms of kidney diseases.

Acknowledgments

Grants

This research was supported by Mayo Clinic

References

Amin HM, McDonnell TJ, Ma Y, Lin Q, Fujio Y, Kunisada K, et al. Selective inhibition of STAT3 induces apoptosis and G(1) cell cycle arrest in ALK-positive anaplastic large cell lymphoma. Oncogene. 2004; 23:5426–5434. [PubMed: 15184887]

Asou Y, Rittling SR, Yoshitake H, Tsuji K, Shinomiya K, Nifuji A, et al. Osteopontin facilitates angiogenesis, accumulation of osteoclasts, and resorption in ectopic bone. Endocrinology. 2001; 142:1325–1332. [PubMed: 11181551]

Bachar AR, Scheffer L, Schroeder AS, Nakamura HK, Cobb LJ, Oh YK, et al. Humanin is expressed in human vascular walls and has a cytoprotective effect against oxidized LDL-induced oxidative stress. Cardiovasc Res. 2010; 88:360–366. [PubMed: 20562421]

Bentley MD, Rodriguez-Porcel M, Lerman A, Sarafov MH, Romero JC, Pelaez LI, et al. Enhanced renal cortical vascularization in experimental hypercholesterolemia. Kidney Int. 2002; 61:1056–1063. [PubMed: 11849461]

Chade AR, Rodriguez-Porcel M, Grande JP, Krier JD, Lerman A, Romero JC, et al. Distinct renal injury in early atherosclerosis and renovascular disease. Circulation. 2002; 106:1165–1171. [PubMed: 12196346]

Chade AR, Rodriguez-Porcel M, Grande JP, Zhu X, Sica V, Napoli C, et al. Mechanisms of renal structural alterations in combined hypercholesterolemia and renal artery stenosis. Arterioscler Thromb Vasc Biol. 2003; 23:1295–1301. [PubMed: 12750121]

Chade AR, Herrmann J, Zhu X, Krier JD, Lerman A, Lerman LO. Effects of proteasome inhibition on the kidney in experimental hypercholesterolemia. J Am Soc Nephrol. 2005a; 16:1005–1012. [PubMed: 15716331]

Chade AR, Lerman A, Lerman LO. Kidney in early atherosclerosis. Hypertension. 2005b; 45:1042–1049. [PubMed: 15897370]

Chade AR, Zhu X, Mushin OP, Napoli C, Lerman A, Lerman LO. Simvastatin promotes angiogenesis and prevents microvascular remodeling in chronic renal ischemia. FASEB J. 2006; 20:1706–1708. [PubMed: 16790524]

Chade AR, Krier JD, Galili O, Lerman A, Lerman LO. Role of renal cortical neovascularization in experimental hypercholesterolemia. Hypertension. 2007; 50:729–736. [PubMed: 17635852]

Collins AJ, Li S, Gilbertson DT, Liu J, Chen SC, Herzog CA. Chronic kidney disease and cardiovascular disease in the Medicare population. Kidney Int Suppl. 2003:S24–S31. [PubMed: 14531770]

Dandapat A, Hu C, Sun L, Mehta JL. Small concentrations of oxLDL induce capillary tube formation from endothelial cells via LOX-1-dependent redox-sensitive pathway. Arterioscler Thromb Vasc Biol. 2007; 27:2435–2442. [PubMed: 17717293]

Guo B, Zhai D, Cabezas E, Welsh K, Nouraini S, Satterthwait AC, et al. Humanin peptide suppresses apoptosis by interfering with Bax activation. Nature. 2003; 423:456–461. [PubMed: 12732850]

Hashimoto Y, Niikura T, Tajima H, Yasukawa T, Sudo H, Ito Y, et al. A rescue factor abolishing neuronal cell death by a wide spectrum of familial Alzheimer's disease genes and Abeta. Proc Natl Acad Sci U S A. 2001; 98:6336–6341. [PubMed: 11371646]

Hoang PT, Park P, Cobb LJ, Paharkova-Vatchkova V, Hakimi M, Cohen P, et al. The neurosurvival factor Humanin inhibits beta-cell apoptosis via signal transducer and activator of transcription 3 activation and delays and ameliorates diabetes in nonobese diabetic mice. Metabolism. 2010; 59:343–349. [PubMed: 19800083]

Ikonen M, Liu B, Hashimoto Y, Ma L, Lee KW, Niikura T, et al. Interaction between the Alzheimer's survival peptide humanin and insulin-like growth factor-binding protein 3 regulates cell survival and apoptosis. Proc Natl Acad Sci U S A. 2003; 100:13042–13047. [PubMed: 14561895]

Ligresti G, Aplin AC, Zorzi P, Morishita A, Nicosia RF. Macrophage-derived tumor necrosis factor-alpha is an early component of the molecular cascade leading to angiogenesis in response to aortic injury. Arterioscler Thromb Vasc Biol. 2011; 31:1151–1159. [PubMed: 21372301]

Miao J, Zhang W, Yin R, Liu R, Su C, Lei G, et al. S14G-Humanin ameliorates Abeta25-35-induced behavioral deficits by reducing neuroinflammatory responses and apoptosis in mice. Neuropeptides. 2008; 42:557–567. [PubMed: 18929410]

Moreno PR, Purushothaman KR, Zias E, Sanz J, Fuster V. Neovascularization in human atherosclerosis. Curr Mol Med. 2006; 6:457–477. [PubMed: 16918368]

Moulton KS, Vakili K, Zurakowski D, Soliman M, Butterfield C, Sylvin E, et al. Inhibition of plaque neovascularization reduces macrophage accumulation and progression of advanced atherosclerosis. Proc Natl Acad Sci U S A. 2003; 100:4736–4741. [PubMed: 12682294]

Oberg BP, McMenamin E, Lucas FL, McMonagle E, Morrow J, Ikizler TA, et al. Increased prevalence of oxidant stress and inflammation in patients with moderate to severe chronic kidney disease. Kidney Int. 2004; 65:1009–1016. [PubMed: 14871421]

Oh YK, Bachar AR, Zacharias DG, Kim SG, Wan J, Cobb LJ, et al. Humanin preserves endothelial function and prevents atherosclerotic plaque progression in hypercholesterolemic ApoE deficient mice. Atherosclerosis. 2011; 219:65–73. [PubMed: 21763658]

Plump AS, Smith JD, Hayek T, Aalto-Setala K, Walsh A, Verstuyft JG, et al. Severe hypercholesterolemia and atherosclerosis in apolipoprotein E-deficient mice created by homologous recombination in ES cells. Cell. 1992; 71:343–353. [PubMed: 1423598]

Salcedo R, Ponce ML, Young HA, Wasserman K, Ward JM, Kleinman HK, et al. Human endothelial cells express CCR2 and respond to MCP-1: direct role of MCP-1 in angiogenesis and tumor progression. Blood. 2000; 96:34–40. [PubMed: 10891427]

Salomonsson L, Pettersson S, Englund MC, Wiklund O, Ohlsson BG. Post-transcriptional regulation of VEGF expression by oxidised LDL in human macrophages. Eur J Clin Invest. 2002; 32:767–774. [PubMed: 12406026]

Scatena M, Liaw L, Giachelli CM. Osteopontin: a multifunctional molecule regulating chronic inflammation and vascular disease. Arterioscler Thromb Vasc Biol. 2007; 27:2302–2309. [PubMed: 17717292]

Sparks MA, Parsons KK, Stegbauer J, Gurley SB, Vivekanandan-Giri A, Fortner CN, et al. Angiotensin II type 1A receptors in vascular smooth muscle cells do not influence aortic remodeling in hypertension. Hypertension. 2011; 57:577–585. [PubMed: 21242463]

Wang J, Ouyang C, Chen X, Fu B, Lu Y, Hong Q. STAT3 inhibits apoptosis of human renal tubular epithelial cells induced by ATP depletion/recovery. Nephron Exp Nephrol. 2008; 108:e11–e18. [PubMed: 18097150]

Wuerzner G, Pruijm M, Maillard M, Bovet P, Renaud C, Burnier M, et al. Marked association between obesity and glomerular hyperfiltration: a cross-sectional study in an African population. Am J Kidney Dis. 2010; 56:303–312. [PubMed: 20538392]

Yeh CH, Chiang HS, Lai TY, Chien CT. Unilateral ureteral obstruction evokes renal tubular apoptosis via the enhanced oxidative stress and endoplasmic reticulum stress in the rat. Neurourol Urodyn. 2011; 30:472–479. [PubMed: 21305585]

Zacharias DG, Kim SG, Massat AE, Bachar AR, Oh YK, Herrmann J, et al. Humanin, a Cytoprotective Peptide, Is Expressed in Carotid Artherosclerotic Plaques in Humans. PLoS ONE. 2012; 7:e31065. [PubMed: 22328926]

Zhu XY, Rodriguez-Porcel M, Bentley MD, Chade AR, Sica V, Napoli C, et al. Antioxidant intervention attenuates myocardial neovascularization in hypercholesterolemia. Circulation. 2004; 109:2109–2115. [PubMed: 15051643]

Zhu XY, Chade AR, Krier JD, Daghini E, Lavi R, Guglielmotti A, et al. The chemokine monocyte chemoattractant protein-1 contributes to renal dysfunction in swine renovascular hypertension. J Hypertens. 2009; 27:2063–2073. [PubMed: 19730125]

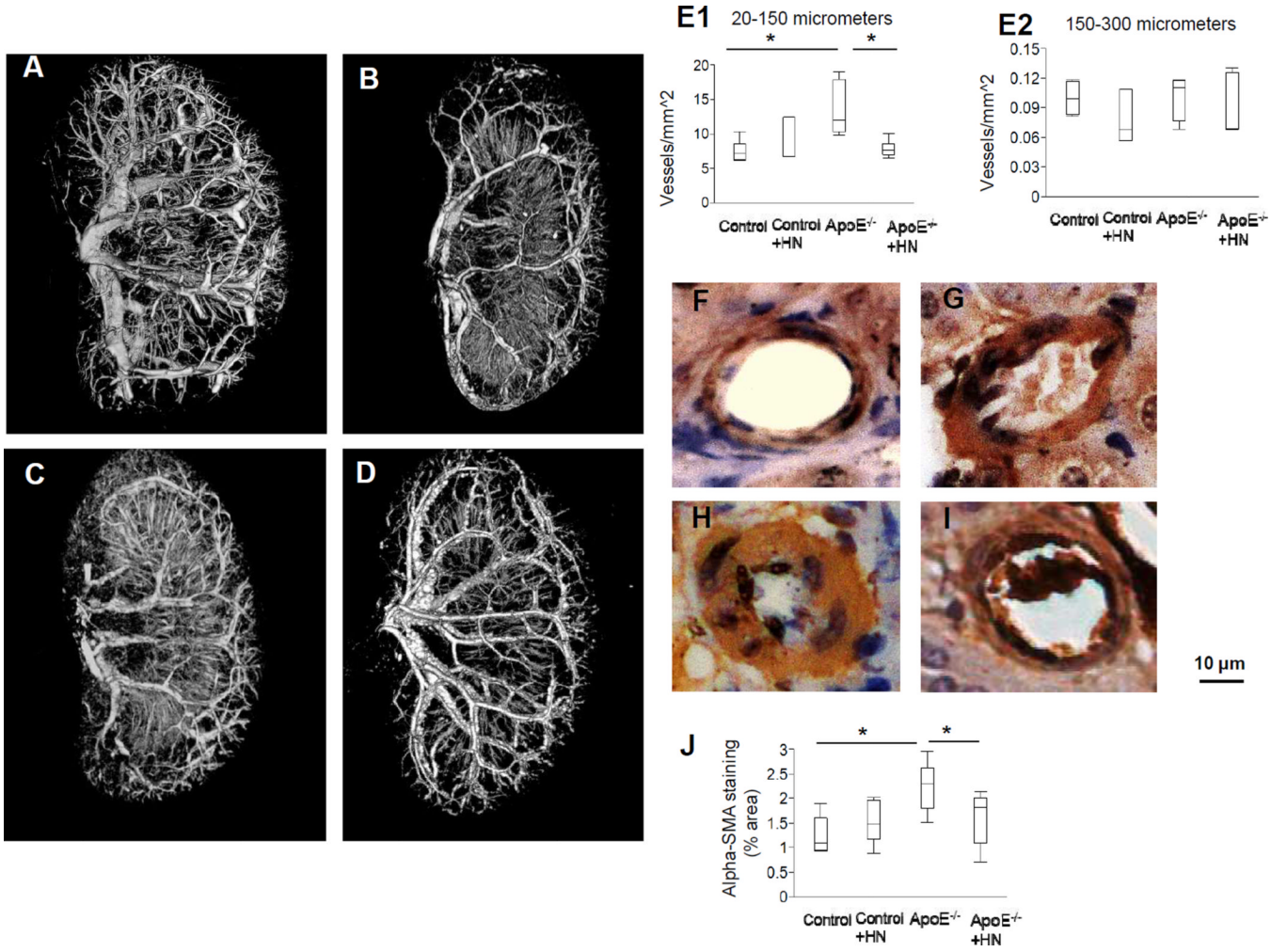

Figure 1.

Renal microvascular density and remodeling. **A–D:** Representative 3-dimensional micro-CT images of the kidney of C57BL/6 mice treated with saline (Control, A) or Humanin (Control +HN, B), or ApoE$^{-/-}$ hypercholesterolemic mice treated with saline (ApoE$^{-/-}$, C) or Humanin (ApoE$^{-/-}$ +HN, D) (n=6 each). **F–I**: Representative images (20x) of renal cortical Alpha-Smooth Muscle Actin (SMA) staining. Cortical microvascular spatial density revealed neovascularization in small microvessels (<150 μm) in ApoE$^{-/-}$, which was normalized by HN **E1**). Vascular remodeling, represented as the ratio of media/lumen areas by alpha-SMA staining, was evident in ApoE$^{-/-}$, but attenuated by HN (**J**). *P<0.05.

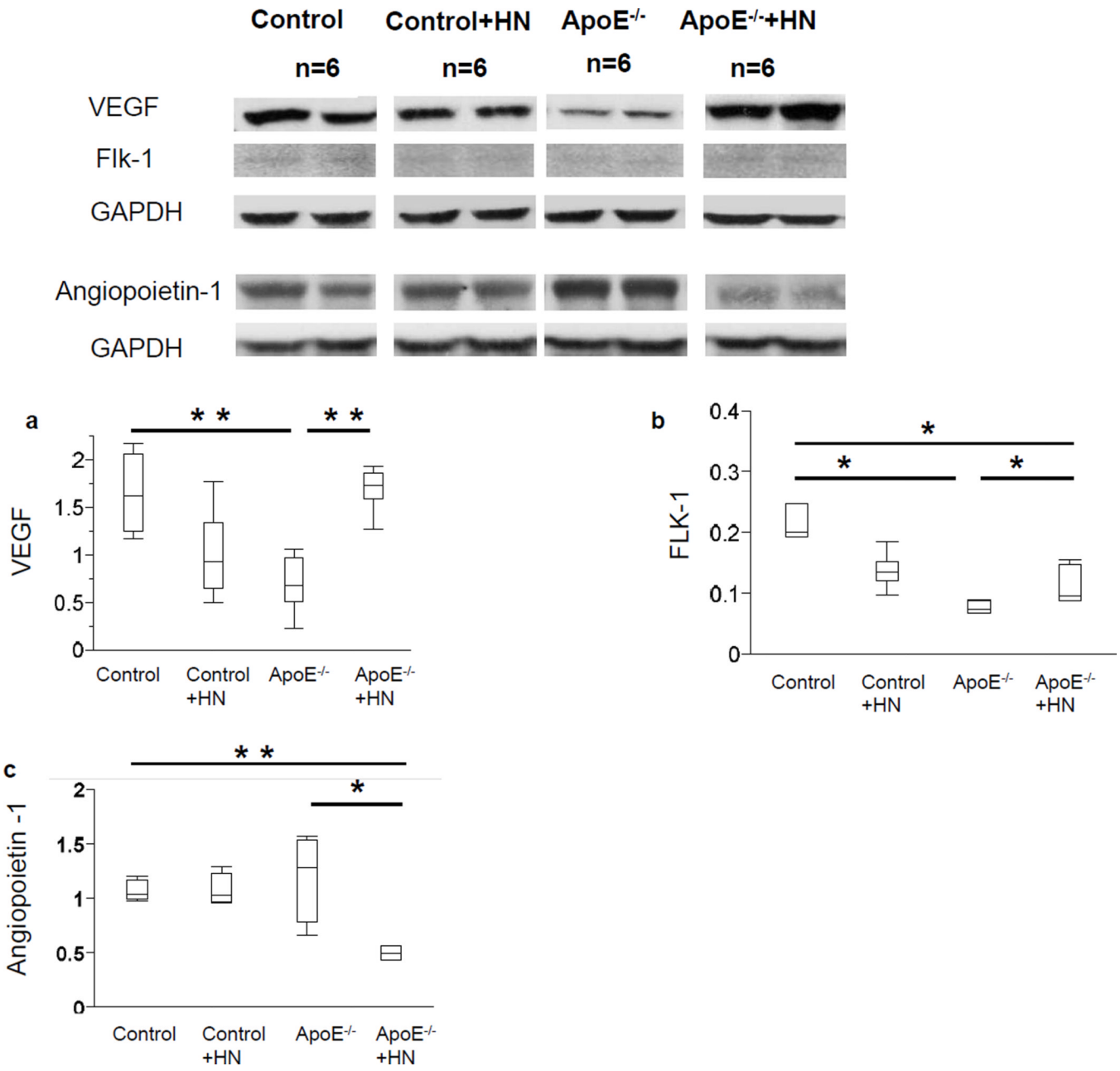

Figure 2.

Renal expressions of angiogenic factors. Vascular endothelial growth factor (VEGF) (a) and VEGF receptor-2 (FLK-1) (b) expression were suppressed in ApoE$^{-/-}$, but improved in ApoE$^{-/-}$+HN. HN inhibited angiopoietin-1(c) in ApoE$^{-/-}$. Quantification of protein bands was relative to GAPDH. *P<0.05, **P<0.01.

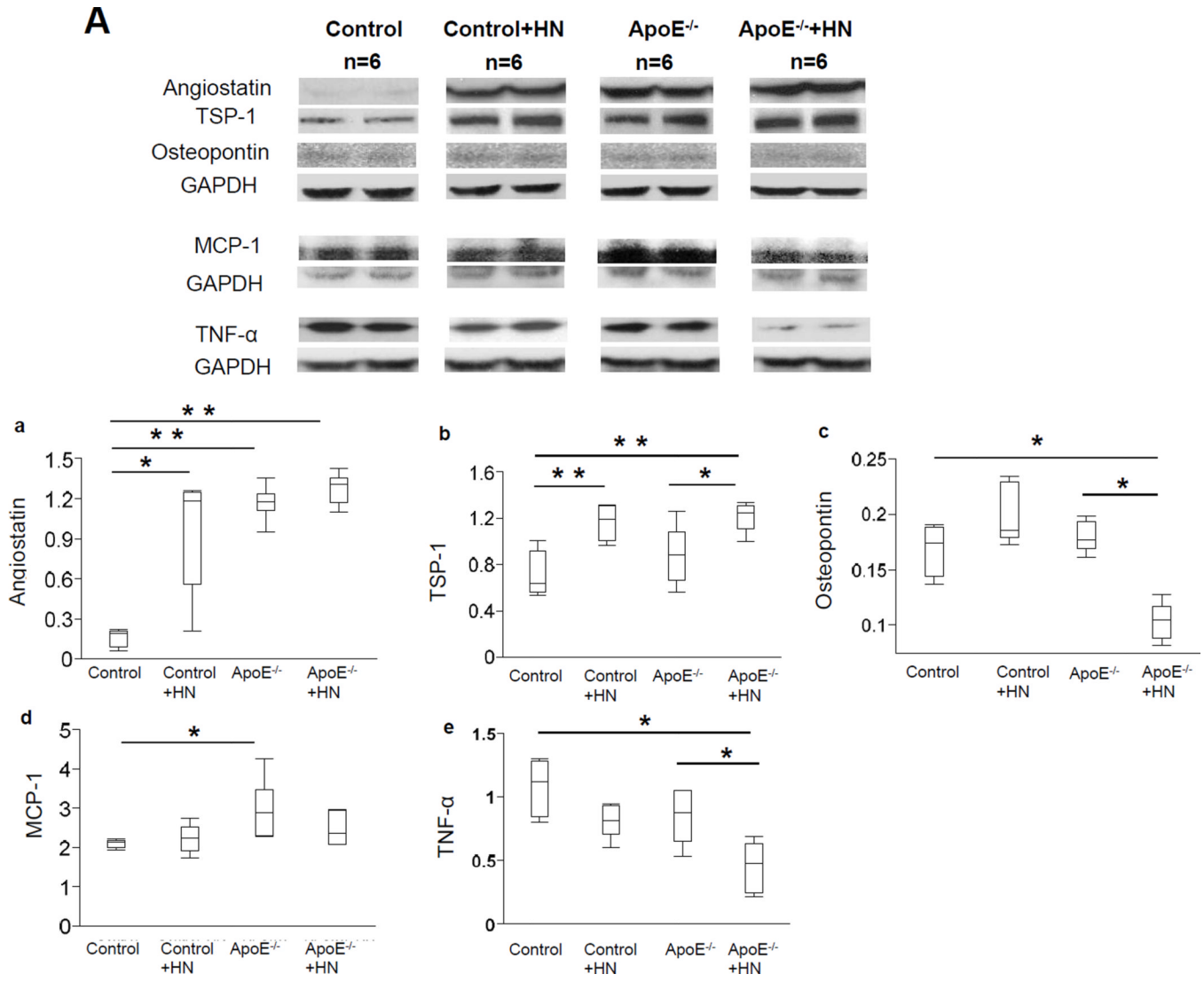

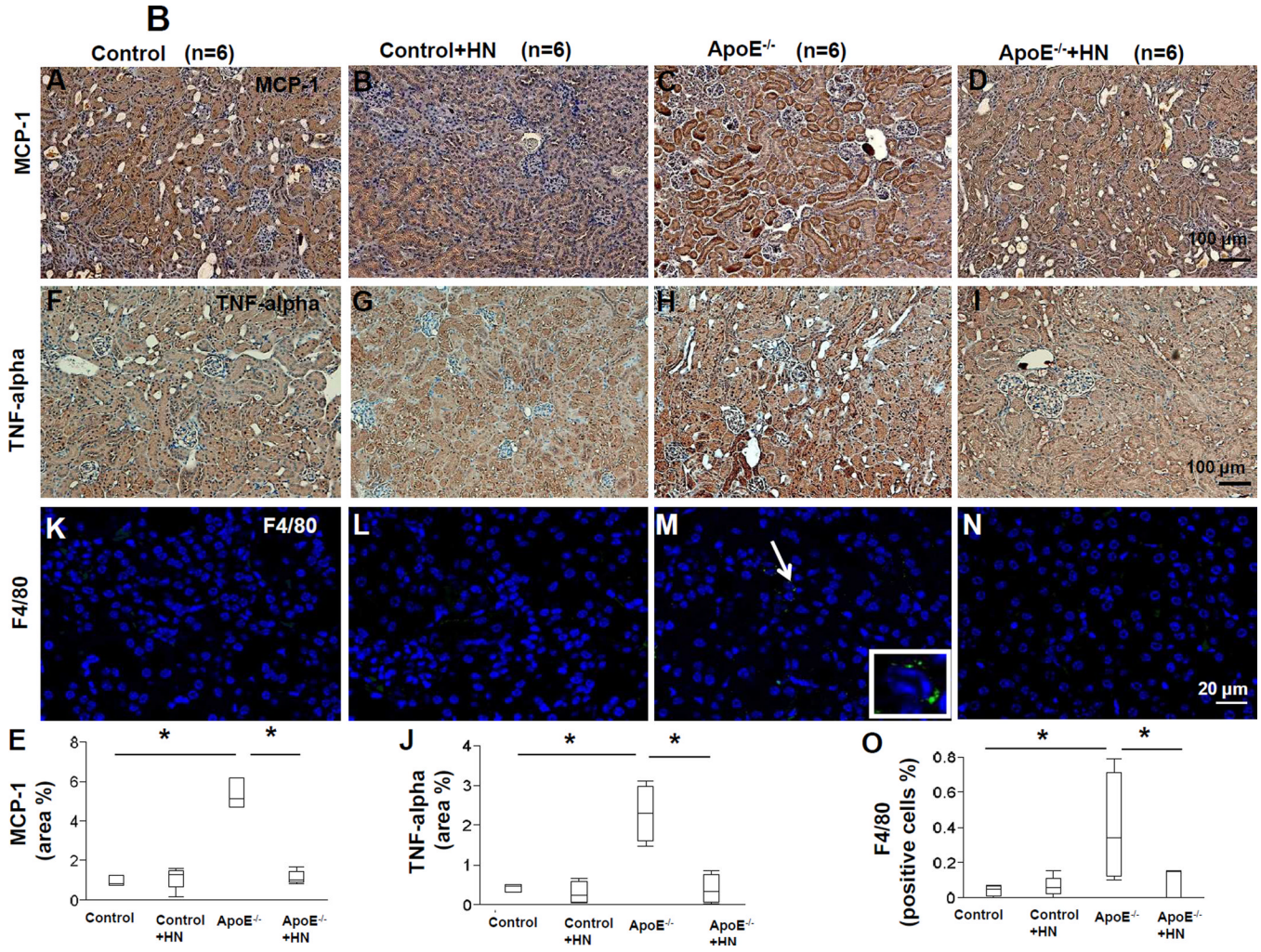

Figure 3.

A. Renal expressions of angiostatic factors and inflammatory markers. Angiostatin (a) and thrombospondin (TSP)-1 (b) were upregulated in both HN-treated groups. HN inhibited osteopontin (c) in ApoE$^{-/-}$. Monocyte chemoattractant protein-1 (MCP-1) (d) was elevated in ApoE$^{-/-}$ and restored by HN, while tumor necrosis factor (TNF)-alpha (e) was inhibited in ApoE$^{-/-}$+HN compared to both control and ApoE$^{-/-}$. Protein bands were quantified relative to GAPDH. *P<0.05, **P<0.01.

B. Renal expressions of inflammatory cytokines and macrophages. Representative images of MCP-1(10x) (A-D), TNF-alpha (10x) (F-I), and F4/80 macrophages (40x) (K-N) in the renal cortex of C57BL/6 mice treated with saline (Control) or Humanin (Control+HN), and ApoE$^{-/-}$ hypercholesterolemic mice treated with saline (ApoE$^{-/-}$) or Humanin (ApoE$^{-/-}$ +HN) (n=6 each). Cortical MCP-1 and TNF-alpha expression were both increased in tubules and to a lesser degree in glomeruli, but restored by HN. Consistently, F4/80 + cells (green), representing macrophages, were abundant in ApoE$^{-/-}$ but normalized by HN. Blue nuclei: DAPI stain. *P<0.05 as indicated.

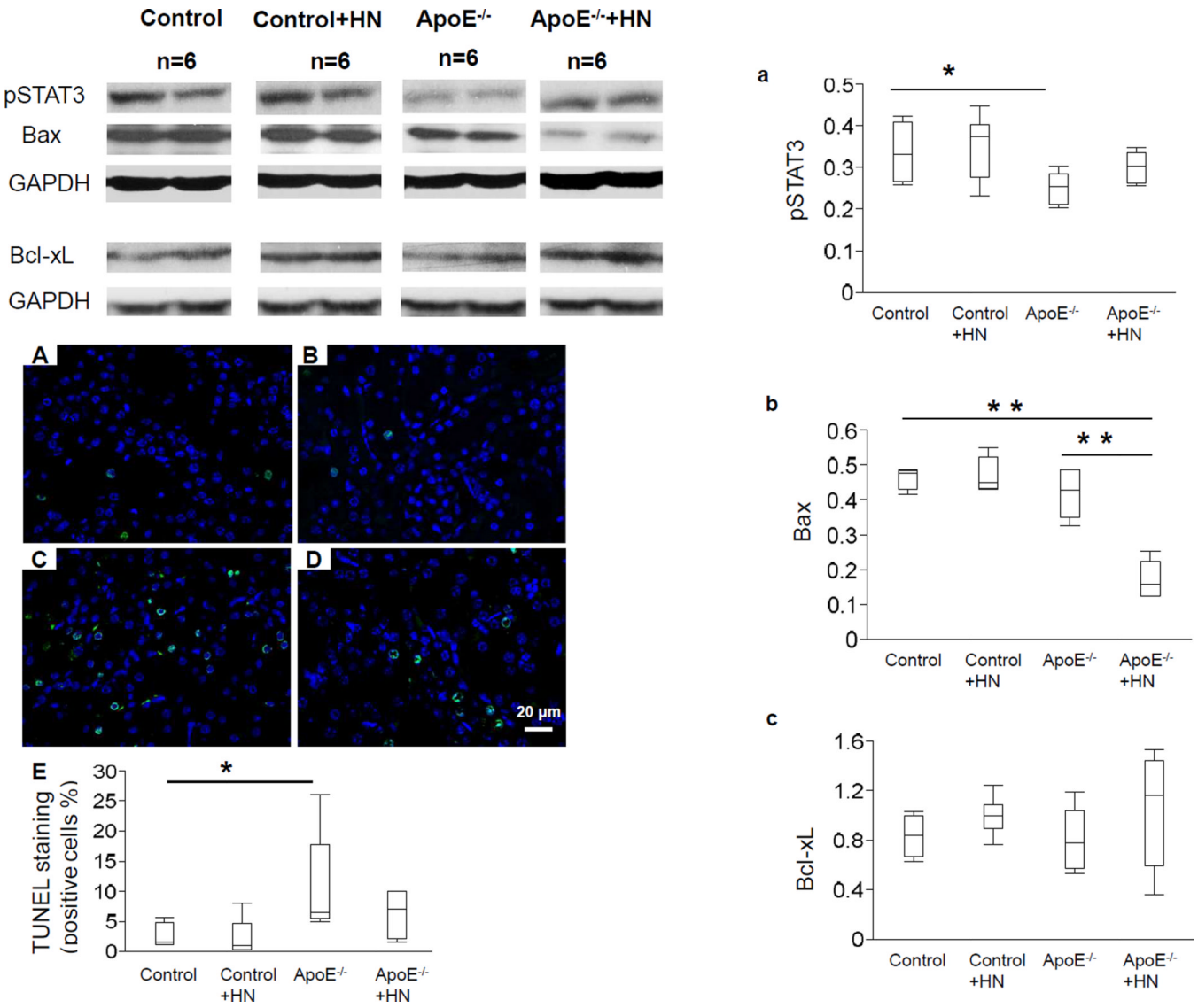

Figure 4.

Renal apoptosis activity and expression of apoptosis-relevant proteins. pSTAT3 (a) was suppressed in ApoE$^{-/-}$ but not in HN, while Bax (b) was inhibited only in ApoE$^{-/-}$ +HN. Bcl-xL (c) was not different among the groups. Quantification of protein bands was relative to GAPDH. **A–D:** Representative images of kidney TUNEL staining (green, 40x) in Control, Control+HN, ApoE$^{-/-}$, and ApoE$^{-/-}$ +HN mice, respectively. **E:** A significant increase in the number of apoptotic cells (TUNEL+, mainly tubulo-interstitial area) was observed in ApoE$^{-/-}$ compared to Control, but not in ApoE$^{-/-}$ +HN. *P<0.05, **P<0.01.

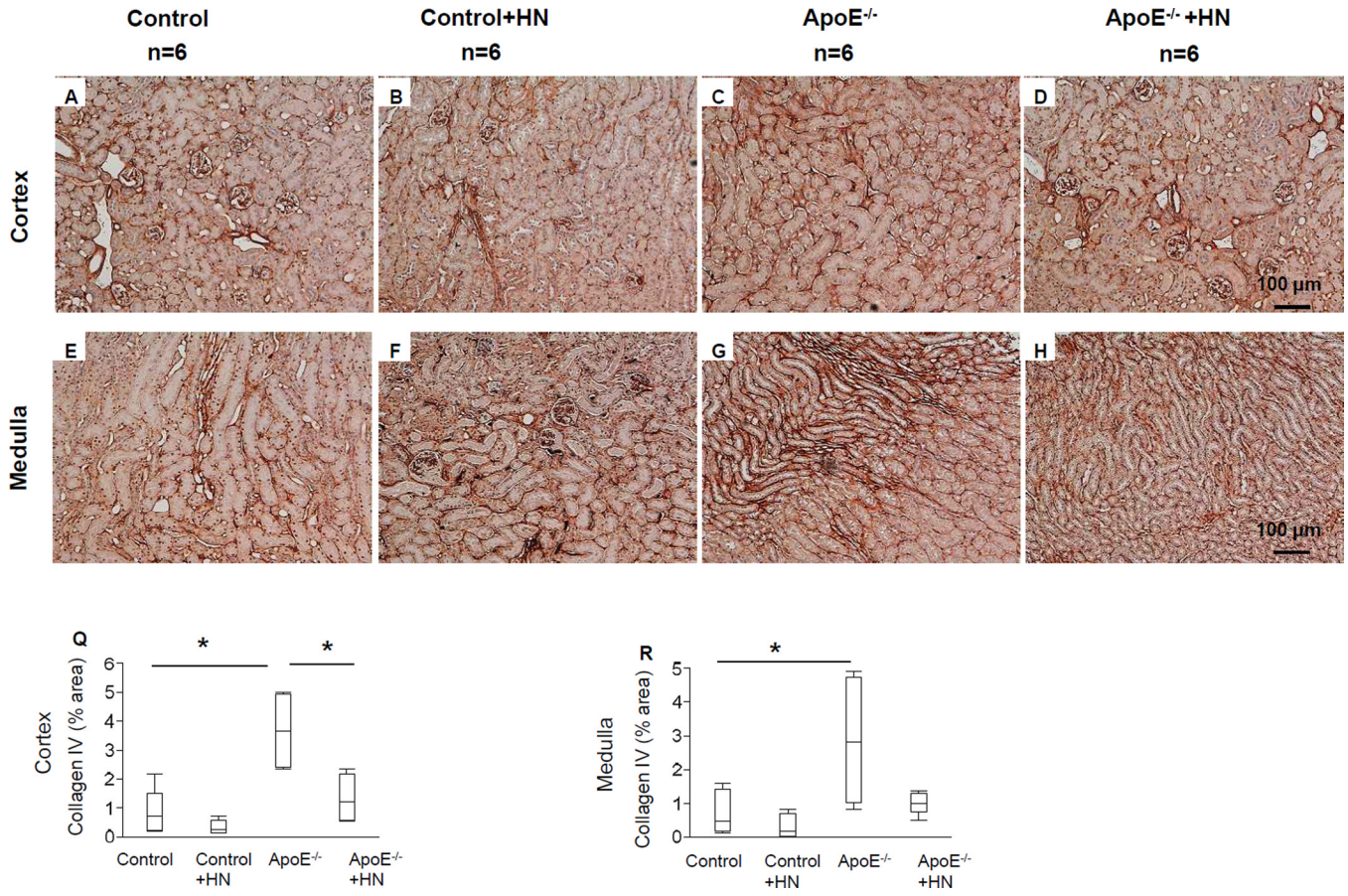

Figure 5.

Renal collagen IV expressions. Representative collagen IV staining (10x) of the renal cortex (**A–D**) and medulla (**E–H**) from C57BL/6 mice treated with saline (Control) or Humanin (Control+HN), and ApoE$^{-/-}$ hypercholesterolemic mice treated with saline (ApoE$^{-/-}$) or Humanin (ApoE$^{-/-}$ +HN), respectively (n=6 each). Collagen IV expression increased in renal cortex (Q) but restored by HN. Collagen IV expression was also increased in medulla (R) in ApoE$^{-/-}$ but not in ApoE$^{-/-}$ +HN. *P<0.05 as indicated.

Table 1

Characteristics (**means± SEM**) of Control mice, or ApoE$^{-/-}$ mice fed a high cholesterol diet, and treated with saline or Humanin (HN).

Characteristics	**Control (n=6)**	**Control+HN (n=6)**	**ApoE$^{-/-}$ (n=6)**	**ApoE$^{-/-}$+HN (n=6)**
Body Weight (g)	20.75±0.76	21.70±0.09	24.28±0.75 **	24.15±0.52 **
Total cholesetol (mg/dl)	64.50± 3.97	69.5 ± 3.80	1092.50 ± 97.86 **	1098.25 ± 109.64 **
Triglyceride (mg/dl)	70.00 ± 8.30	67.5 ± 6.28	81.00 ± 5.12	105.00 ± 20.24
Creatinine (mg/dl)	0.15 ± 0.02	0.20 ± 0.02	0.10 ± 0.02	0.11 ± 0.04
BUN (mg/dl)	34.30 ± 2.63	32.33 ± 0.97	44.94 ± 3.40 *	43.82 ± 2.36 *
PRC (U/μl)	14.6 ± 2.3	17.6 ± 5.4	8.2 ± 3.8 ^	17.8 ± 1.3

BUN, blood urea nitrogen; PRC, plasma renin concentration.

* P<0.05 compared to Controls;

** P<0.01 compared to Controls;

^ P<0.05 compared to ApoE$^{-/-}$+HN.